arXiv:0912.2633v1 [cond-mat.mtrl-sci] 14 Dec 2009

Ab initio investigation of $\mathrm{Fe}^{2+}/\mathrm{Fe}^{3+}$ dimerization and ferroelectricity in multiferroic magnetite: role of electronic correlations

Tetsuya Fukushima, Kunihiko Yamauchi, and Silvia Picozzi[*]
Consiglio Nazionale delle Ricerche - Instituto Nazionale di Fisica della Materia (CNR-INFM),
CASTI Regional Lab., 67100 L'Aquila, Italy

(Dated: December 14, 2009)

Based on *ab initio* density functional theory, we have investigated a microscopic mechanism that leads to $\mathrm{Fe}_{\mathrm{B}}^{2+}/\mathrm{Fe}_{\mathrm{B}}^{3+}$ dimerization and consequent ferroelectricity in charge ordered $\mathrm{Fe_3O_4}$ with $P2$ symmetry. In addition to the simple inter-site Coulomb repulsion, quantum hybridization effects are invoked to explain the $\mathrm{Fe}_{\mathrm{B}}^{2+}/\mathrm{Fe}_{\mathrm{B}}^{3+}$ bond dimerization. Our results, based on the generalized gradient approximation + Hubbard U (GGA+U) method, indicate that noncentrosymmetric $P2$ magnetite shows a finite and sizeable ferroelectric polarization along the b crystalline axis. From the U dependence of polarization, we conclude that the origin of ferroelectricity in $P2$ $\mathrm{Fe_3O_4}$ lies in the recently proposed "intermediate site/bond-centered charge ordering".

PACS numbers: 75.50.Gg, 77.80.-e

I. INTRODUCTION

Advanced multifunctional materials showing coexisting and spontaneous long-range dipolar and magnetic orders are nowadays referred to as *multiferroics* [1]; they combine extremely fascinating physics phenomena with a huge potential for technological applications. Recently, large interests have been devoted to *improper* multiferroics [1, 2]: here, ferroelectricity is driven by unconventional mechanisms, such as the loss of centrosymmetry due to the occurrence of long-range *spin* or *charge* order (at variance with more conventional ferroelectrics in which the ionic degrees of freedom play a prominent role in inducing permanent dipole moments).

Magnetite, $\mathrm{Fe_3O_4}$ (formally $\mathrm{Fe}_{\mathrm{A}}^{3+}[\mathrm{Fe}^{2.5+}\mathrm{Fe}^{2.5+}]_{\mathrm{B}}\mathrm{O}_4^{2-}$), crystallizes in the inverted cubic spinel structure $Fd\bar{3}m$ and shows a metallic behavior at room temperature. $\mathrm{Fe_A}$ and $\mathrm{Fe_B}$ ion sites are coordinated to O ions in the inverted spinel structure $\mathrm{Fe_3O_4}$, *i.e.,* the tetrahedrally surrounded Fe sites are occupied by $\mathrm{Fe_A}$ atoms, whereas the octahedrally coordinated Fe sites are occupied by $\mathrm{Fe_B}$ atoms. The latter form a pyrochlore lattice, which consists of a network of corner sharing tetrahedra. Ferrimagnetism is stable in $\mathrm{Fe_3O_4}$, with magnetic moments of $\mathrm{Fe_A}$ sites antiparallel to those of $\mathrm{Fe_B}$ sites. $\mathrm{Fe_3O_4}$ undergoes a first order metal-insulator transition (called Verwey transition) at around 120 K, where the resistivity of $\mathrm{Fe_3O_4}$ increases by two orders of magnitude. [3] This phase transition accompanies a change in the crystal structure of $\mathrm{Fe_3O_4}$, from cubic to monoclinic symmetry. Verwey proposed that the metal-insulator transition originates from a charge ordering at the $\mathrm{Fe_B}$ sites ($\mathrm{Fe}_{\mathrm{A}}^{3+}[\mathrm{Fe}^{2+}\mathrm{Fe}^{3+}]_{\mathrm{B}}\mathrm{O}_4^{2-}$), similar to strongly correlated hole-doped manganites. [4] A full charge localization with ideal $\mathrm{Fe}_{\mathrm{B}}^{2+}$ and $\mathrm{Fe}_{\mathrm{B}}^{3+}$ does not occur, since the charge disproportionation is much smaller than the ideal 3+/4+ ionic picture, due to strong covalency effects. Anderson pointed out that, when putting two Fe^{2+} and two Fe^{3+} on each $\mathrm{Fe_B}$ tetrahedron, the number of Fe^{2+} and Fe^{3+} pairs is maximized and this gives rise to the lowest energy from the Coulomb repulsion point of view. [5] However, the Anderson criterion for low temperature $\mathrm{Fe_3O_4}$ are inconsistent with recent experiment results. [6, 7] As such, the charge ordering occurring at the Verwey transition in $\mathrm{Fe_3O_4}$ is still under discussion.

Ferroelectricity has been recently observed at low temperatures in $\mathrm{Fe_3O_4}$ and attracted great scientific interests. [8, 9] Khomskii *et al.* have proposed that $\mathrm{Fe_3O_4}$ might show ferroelectricity by means of an intermediate site/bond-centered charge ordering, being one of the first multiferroic materials. [10] We investigated ferroelectricity in $\mathrm{Fe_3O_4}$ by *ab initio* calculations, as showing that magnetite has non-centrosymmetric Cc symmetry structure in the ground state and the origin of ferroelectricity in $\mathrm{Fe_3O_4}$ is not the site/bond-centered charge ordering, but a "charge shift" between specific $\mathrm{Fe_B}$ site. [11]

In contrast to our previous study, in this paper we focus on noncentrosymmetric $P2$ (No.3) structure in order to realize the picture proposed by Khomskii, where the ferroelectric polarization arises from the $\mathrm{Fe}_{\mathrm{B}}^{2+}/\mathrm{Fe}_{\mathrm{B}}^{3+}$ dimerization. We elucidate three physical properties in $\mathrm{Fe_3O_4}$ based on *ab initio* density functional theory. The first point is a mechanism for $\mathrm{Fe}_{\mathrm{B}}^{2+}/\mathrm{Fe}_{\mathrm{B}}^{3+}$ dimerization along the monoclinic b direction. Our results indicate that the hybridization of electronic orbitals between $\mathrm{Fe}_{\mathrm{B}}^{2+}$ sites (*i.e.* a quantum mechanical effect) is as important as the classical inter-site Coulomb interactions for the $\mathrm{Fe}_{\mathrm{B}}^{2+}/\mathrm{Fe}_{\mathrm{B}}^{3+}$ bond dimerization. The second point is related to ferroelectricity in $P2$ $\mathrm{Fe_3O_4}$ as induced by intermediate site/bond-centered charge ordering proposed by Khomskii *et. al.* [10] Ferroelectric polarizations (calculated via the Berry-phase approach) are compared to those obtained in Ref.[11] for Cc magnetite. Finally, we investigate the stability of antiferroelectric $P2/c$ (No.13)

---

[*] Electronic address: silvia.picozzi@aquila.infn.it

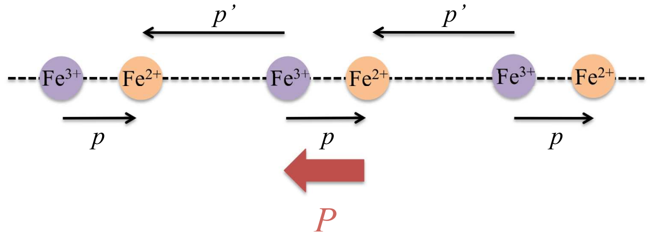

FIG. 1: Illustration of a net polarization (red arrow) by the intermediate site-centered and bond-centered charge ordering in Fe_3O_4. The Fe_B^{2+} and Fe_B^{3+} charge ordering and an alternation of *short* and *long* bond lengths between Fe_B^{2+} and Fe_B^{3+} sites in low temperature magnetite are shown.

and ferroelectric $P2$ Fe_3O_4 vs electronic correlation effects.

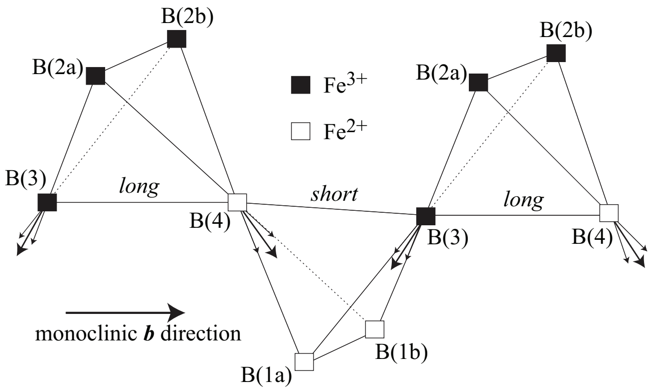

FIG. 2: Schematics of the corner sharing tetrahedra formed by Fe_B sites in $P2/c$ Fe_3O_4. The labels of Fe_B site are consistent with Ref.12. Black and white squares indicates Fe_B^{3+} and Fe_B^{2+} sites, respectively.

II. ELECTRIC POLARIZATION INDUCED BY CHARGE ORDERING: BASIC CONCEPTS

Khomskii *et al.* have discussed how charge ordering could induce ferroelectricity in magnetic systems. [10] According to their idea, when either site-centered or bond-centered charge orderings happen individually, a system does not have a net dipole moment: however, if the site-centered and bond-centered charge orderings occur simultaneously in a system, the inversion symmetry is broken so that the system shows a net dipole moment, therefore becoming ferroelectric (*cf.* Fig.1). [10] Based on this scenario, Khomskii *et al.* have proposed that Fe_3O_4 could become ferroelectric, with the monoclinic b axis as polarization direction. Actually, experimental results indicate that the situation in Fe_3O_4 is similar to the intermediate site/bond-centered charge ordering: Wright *et al.* [12] have investigated the crystal structure of Fe_3O_4 at low temperature by using high-resolution neutron powder-diffraction and X-ray powder-diffraction measurements. According to Ref.[12], the distances between charge ordered Fe_B^{2+}/Fe_B^{3+} sites along b are strongly modulated, from 2.86 Å to 3.05 Å. So, in addition to the site-centered charge ordering of Fe_B^{2+} and Fe_B^{3+} sites, there is a sequence of *short* and *long* Fe_B-Fe_B bond lengths along b (*i.e.* bond dimerization process). This situation indeed corresponds to the site/bond-centered charge ordering proposed by Khomskii *et al* [10]., the so called "Zener polaron".

Generally, the origin of bond dimerization in other multiferroic materials is the spin configuration, *e.g.,* in $HoMn_2O_5$ the bond lengths between antiparallel (parallel) Mn ions are expanded (contracted) so as to optimize the double exchange mechanism. [13] There is, however, no correlation between the dimerization process and the spin configuration in Fe_3O_4, since all the spin directions of Fe_B sites are the same. Wright *et al.* have proposed the bond length modulation to be due to the simple classical inter-site Coulomb repulsion between charge ordered Fe_B^{2+} and Fe_B^{3+} sites, *i.e.,* below the Verwey temperature the corner sharing Fe_B tetrahedra are constructed by three Fe_B^{3+} and one Fe_B^{2+} ions or by three Fe_B^{2+} and one Fe_B^{3+} ions (3-1 charge order), at variance with the Anderson criterion in which the configurations of two Fe_B^{2+} and two Fe_B^{3+} ions (2-2 charge order) are most stable [5], as shown in Fig.2. It can be easily understood that a system can lower its energy, from the *inter-site* Coulomb interaction point of view, if Fe_B ions on B(3) and B(4) sites move along the thin arrows in Fig.2. As a result, Fe_B ions on B(3) and B(4) sites are moved along the bold arrows in Fig.2, the net effect being a bond dimerization between B(3) and B(4) sites. However, as we'll show, an important role in the dimerization process in Fe_3O_4 is played by the *on-site* Coulomb interaction of Fe atoms as well, and understanding the dimerization process in Fe_3O_4 is not so trivial.

III. CALCULATION METHOD

Electronic structure calculations and structural optimizations are performed by the "Vienna *Ab initio* Simulation Package" (VASP) and Projector Augmented Wave (PAW) pseudopotentials. [14] The Perdew-Becke-Erzenhof (PBE) of the generalized gradient approximation (GGA) is employed for the exchange-correlation potential. [15] The plane wave cutoff energies are 400 eV for Fe and O atoms. The GGA+U calculations within Dudarev's approach are performed by applying a Hubbard-like potential for Fe-d states only. [16] Effective Coulomb energies U = 4.5, 6.0, and 8.0 eV and an exchange parameter J = 0.89 eV are used. [17] To calculate the electronic structure of ferroelectric Fe_3O_4, we consider an "artificial" crystal structure with $P2$ symmetry, built by copying the lower half of the (experimentally suggested) monoclinic $P2/c$ antiferroelectric cell to the up-

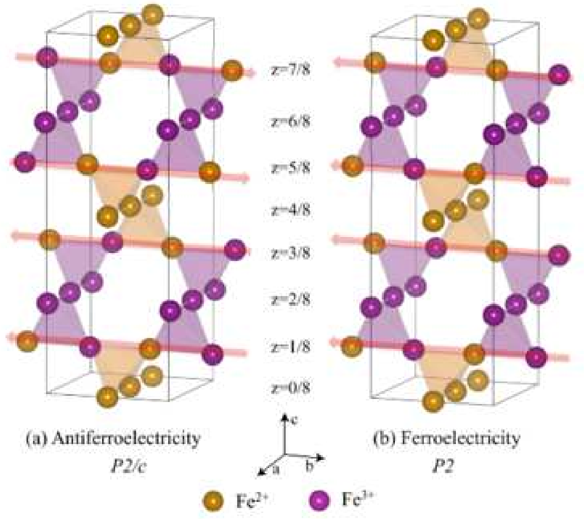

FIG. 3: Red arrows show local polarization directions in (a) antiferroelectric $P2/c$ and (b) ferroelectric $P2$ Fe_3O_4. Purple and orange spheres indicate Fe_B^{3+} and Fe_B^{2+} ions, respectively. For clarity, Fe_A and O ions are not shown. Tetrahedra composed by three Fe_B^{2+} and one Fe_B^{3+} ions and three Fe_B^{3+} and one Fe_B^{2+} ions are highlighted by orange and purple planes, respectively.

per half, as shown in Fig.3. Note that there is no net polarization in antiferroelectric $P2/c$ magnetite, because the local polarizations in the upper half and lower half cancel each other. On the other hand, ferroelectric $P2$ Fe_3O_4 can show a finite net polarization. Computational details for the electronic structure and structural optimization in ferroelectric $P2$ Fe_3O_4 are the same as antiferroelectric $P2/c$. Both $P2/c$ and $P2$ contain 56 atoms (24 Fe and 32 O ions) in $a_c/\sqrt{2}\times a_c/\sqrt{2}\times 2a_c$ unit cell, where a_c stands for the lattice constant of cubic $Fd\bar{3}m$ Fe_3O_4. Lattice parameters are fixed to experimental values: $a = 5.9341$ Å, $b = 5.9256$ Å, $c = 16.7524$ Å, and $\beta = 90.2000°$. [18] In the structural optimization, a threshold on the atomic forces of 0.01 eV/Å is employed. Internal atomic coordinates are optimized in $P2/c$ and $P2$ Fe_3O_4 starting from experimental Wyckoff parameters. [12] Fe-$3p^6 3d^6 4s^2$ and O-$2s^2 2p^4$ electrons are treated as valence electrons. For Fe atoms, the ferrimagnetic configuration is considered: all Fe_A sites have up-spin and all Fe_B sites have down-spin. We neglected spin-orbit coupling, so that the direction of magnetization with respect to the crystal is not specified. For the $P2/c$ and $P2$ Fe_3O_4, the $6\times6\times2$ Monkhost-Pack k-point grid in the Brillouin zone is used. The Berry phase approach [19, 20] within the PAW formalism and the point charge model with nominal charges (Fe_A: 3+, Fe_B^{2+}: 2+, Fe_B^{3+} : 3+, and O: 2-) are employed to calculate polarization. We integrate over six k-point strings parallel to the polarization direction (crystallographic b direction) in the Berry phase approach.

IV. RESULTS

A. Fe^{2+}/Fe^{3+} bond dimerization in Fe_3O_4

First, we will show that the site/bond-centered charge ordering occurs in Fe_3O_4, so that ferroelectricity can be expected. Figure 4 illustrates charge densities (in a selected energy range, see caption) of Fe_B^{2+}, Fe_B^{3+}, and O^{2-} sites in ferroelectric $P2$ Fe_3O_4 and an enlarged view of one of the z=1/8, 3/8, 5/8, and 7/8 planes in Fig.3(b). As discussed in a previous study [21], one electron occupies one of the spin down t_{2g} orbitals (xy, yz, and zx) on Fe^{2+} sites (d^6 configuration, $t_{2g\uparrow}^3 e_{g\uparrow}^2 t_{2g\downarrow}^1$); therefore, charge densities on Fe^{2+} sites have a cross-like shape corresponding to t_{2g} orbitals and extend to interstitial regions of anions O^{2-}. The spin down t_{2g} orbitals on Fe^{3+} sites (d^5 configuration, $t_{2g\uparrow}^3 e_{g\uparrow}^2$) are pushed above the Fermi level. The important point here is the charge density on the O^{2-} sites: charge is not present on O^{2-} sites in the *long* bonds (*cfr.* Fig.4), whereas in the *short* bond sides there is an appreciable charge density with Oxygen p character. The latter can be viewed as"bond-centered charge". It can be easily seen that there is no overlap between d orbitals on Fe_B^{2+} and Fe_B^{3+} sites and p orbitals on O^{2-} sites in the *long* bond sides; however, the d orbitals between Fe_B^{2+} and Fe_B^{3+} sites via p orbitals on O^{2-} sites can hybridize on the *short* bond sides. Note that the hybridization between d orbitals on Fe_B^{2+} sites and p orbitals on O^{2-} sites is not perfectly π-like because of the small tilt of p orbitals on O^{2-} sites, so that we can expect a somewhat larger hybridization with respect to the ideally undistorted atomic arrangement. As a result, due to orbital hybridization, *short* bond sides have higher electron density and *long* bond sides have lower electron density. The center of gravity of charges is therefore expected to move away from the ions and we infer from Fig.4 that, in addition to the *site*-centered charge ordering on Fe_B sites, even the *bond*-centered charge ordering proposed by Khomskii *et al.* is realized in Fe_3O_4. [10]

Table I shows the dependence of Fe_B-Fe_B bond lengths on the on-site Coulomb interaction U in the corner sharing tetrahedra and valence charges q_d of Fe_B sites in ferroelectric $P2$ Fe_3O_4 (the numbering of Fe_B sites corresponds to that of $P2/c$ structure in Fig.2). As shown in

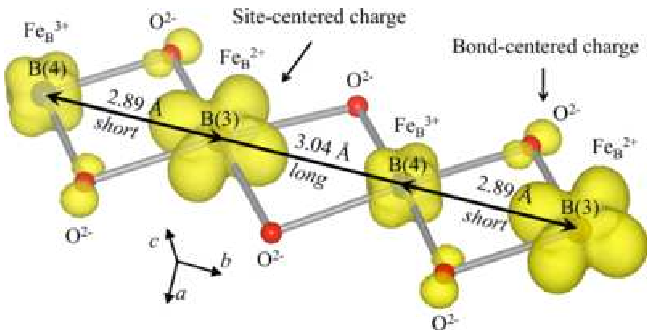

FIG. 4: Minority-spin charge densities of $\mathrm{Fe}_{\mathrm{B}}^{2+}$, $\mathrm{Fe}_{\mathrm{B}}^{3+}$, and O^{2-} sites in ferroelectric $P2$ $\mathrm{Fe_3O_4}$. A closeup of one of the z=1/8, 3/8, 5/8, and 7/8 planes in Fig.3(b). *Short* and *long* mean alternations of bond lengths between $\mathrm{Fe_B}$ sites due to the $\mathrm{Fe}^{3+}/\mathrm{Fe}^{2+}$ bond dimerization along b. Charge densities are calculated within 1.00 eV below the Fermi level.

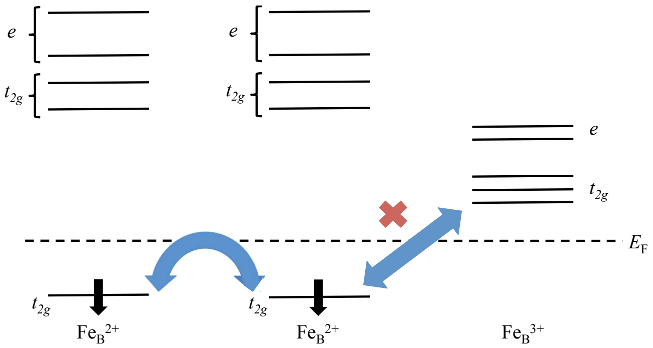

FIG. 5: Schematics of "asymmetric hybridization" between $\mathrm{Fe}_{\mathrm{B}}^{2+}$ sites in the minority spin state. Thin black arrows denote the electron spin and thick blue arrows indicate electron hopping.

the upper part of Table I and Fig.2, there are alternations of *short* and *long* bond lengths between $\mathrm{Fe_B}$ sites, leading to the $\mathrm{Fe}^{2+}/\mathrm{Fe}^{3+}$ bond dimerization along the b axis, so that the corner sharing tetrahedra formed by $\mathrm{Fe_B}$ sites are strongly distorted from ideal regular tetrahedra. Table I also indicates that the distortions of the tetrahedra are suppressed upon increasing U. For example, along the b direction, the bond lengths between $\mathrm{Fe_B}(3)$ and $\mathrm{Fe_B}(4)$ sites are modulated from 2.888 to 3.038 Å for U=4.0 eV, from 2.919 to 3.006 Å for U=6.0 eV, and from 2.934 to 2.992 Å for U=8.0 eV, respectively (the bond length is modulated from 2.880 to 3.046 Å in the experiment [7]).

Now, we focus on a mechanism of the $\mathrm{Fe}^{2+}/\mathrm{Fe}^{3+}$ bond dimerization in $\mathrm{Fe_3O_4}$. Previous studies [12, 17] suggested dimerization on $\mathrm{Fe}_{\mathrm{B}}^{2+}$ and $\mathrm{Fe}_{\mathrm{B}}^{3+}$ sites to originate from the inter-site Coulomb interaction between $\mathrm{Fe_B}$ sites. However, this is not the only factor and we propose that "asymmetric hybridization" plays a relevant role in this context (*cfr.* Fig. 5). As mentioned above, one electron occupies the t_{2g} down spin states at $\mathrm{Fe}_{\mathrm{B}}^{2+}$ sites, whereas t_{2g} and e_g down spin states at $\mathrm{Fe}_{\mathrm{B}}^{3+}$ sites are located above the Fermi level. In such conditions, $\mathrm{Fe}_{\mathrm{B}}^{2+}$ electron orbitals can hybridize, so that the $\mathrm{Fe}_{\mathrm{B}}^{2+}$-$\mathrm{Fe}_{\mathrm{B}}^{2+}$ bond lengths are shrinked. However, electron orbitals on $\mathrm{Fe}_{\mathrm{B}}^{2+}$ and $\mathrm{Fe}_{\mathrm{B}}^{3+}$ sites hybridize much less, due to the larger energy level difference between the t_{2g} down spin states in $\mathrm{Fe}_{\mathrm{B}}^{2+}$ and $\mathrm{Fe}_{\mathrm{B}}^{3+}$ sites; therefore, shortening of bond lengths between $\mathrm{Fe}_{\mathrm{B}}^{2+}$ and $\mathrm{Fe}_{\mathrm{B}}^{3+}$ sites can not be expected by orbital hybridization. In this sense, we refer to the hybridization of electron orbitals on $\mathrm{Fe}_{\mathrm{B}}^{2+}$ sites in $\mathrm{Fe_3O_4}$ as "asymmetric hybridization".

In order to prove the validity of the "asymmetric hybridization", we investigate the on-site Coulomb interaction dependence of valence charges q_d of $\mathrm{Fe_B}$ ions (calculated within a Wigner-Seitz radius $r = 1.00$Å). As shown in the lower part of Table I, the $\mathrm{Fe}_{\mathrm{B}}^{2+}/\mathrm{Fe}_{\mathrm{B}}^{3+}$ charge ordering occurs in $\mathrm{Fe_3O_4}$. This $\mathrm{Fe}_{\mathrm{B}}^{2+}/\mathrm{Fe}_{\mathrm{B}}^{3+}$ charge ordering has been well known and investigated. [17] We note that, when U is set to zero, there is neither charge order nor bond dimerization of $\mathrm{Fe_B}$ sites, due to metallicity. The key point here is the U dependence of charge separations between $\mathrm{Fe_B}$ sites. Our results indicate that, upon increasing U, the charge separation in $\mathrm{Fe_B}$ sites increases, due to the fact that electrons are more localized for large U. Therefore, upon increasing the charge separations in $\mathrm{Fe_B}$ sites, one expects the inter-site Coulomb interactions to more strongly distort the $\mathrm{Fe_B}$ tetrahedra, implying a larger tendency towards bond dimerization between $\mathrm{Fe_B}$ sites. However, Table I shows that the dimerization on $\mathrm{Fe_B}$ sites decreases when increasing U. We infer that these results can not be explained by inter-site Coulomb interaction only. Indeed, from the "asymmetric hybridization" point of view, it can be expected that, due to the stronger localization of electrons for large U, the reduced hybridization leads to a weakening of dimerization on $\mathrm{Fe_B}$ sites (as confirmed by Table I).

B. Ferroelectricity in $\mathrm{Fe_3O_4}$

From the discussion in the previous section, we can expect ferroelectric polarization along b in $P2$ $\mathrm{Fe_3O_4}$ to occur by means of the site/bond-centered charge proposed by Khomskii *et. al.* [10] Due to the presence of inversion symmetry, $P2/c$ $\mathrm{Fe_3O_4}$ doesn't have a net polarization; however, there is no inversion symmetry in $P2$ $\mathrm{Fe_3O_4}$, so the system is allowed to have finite polarization. We choose the antiferroelectric $P2/c$ $\mathrm{Fe_3O_4}$ as a centrosymmetric reference structure, *i.e.,* spontaneous polarization is obtained by polarization difference between ferroelectric $P2$ and antiferroelectric $P2/c$ $\mathrm{Fe_3O_4}$, $\Delta P = P_{\mathrm{FE}} - P_{\mathrm{AFE}}$. Here, polarization along b in $\mathrm{Fe_3O_4}$ is calculated by two different methods: one is the Berry phase method, where the macroscopic polarization is obtained from the Wannier-center displacements, [19] another is the simple "point charge model" with nominal charges on the Fe an O ions. Note that the polariza-

U (eV)	B(1a)-B(1b)	B(1a)-B(3)	B(1a)-B(4)	B(1b)-B(3)	B(1b)-B(4)	B(2a)-B(2b)
4.5	2.9671	2.9215	2.9129	2.9118	2.9046	2.9671
6.0	2.9671	2.9169	2.9366	2.9067	2.9289	2.9671
8.0	2.9671	2.9156	2.9510	2.9058	2.9431	2.9671
U (eV)	B(2a)-B(3)	B(2a)-B(4)	B(2b)-B(3)	B(2b)-B(4)	B(3)-B(4)	B(4)-B(3)
4.5	3.0028	3.0195	3.0091	3.0247	**3.0379**	**2.8877**
6.0	2.9958	3.0080	3.0017	3.0129	**3.0064**	**2.9193**
8.0	2.9920	2.9977	2.9984	3.0031	**2.9923**	**2.9336**
U (eV)	B(1a)	B(1b)	B(2a)	B(2b)	B(3)	B(4)
4.5	5.373	5.372	5.140	5.140	5.166	5.358
6.0	5.398	5.397	5.106	5.106	5.116	5.401
8.0	5.413	5.412	5.073	5.073	5.077	5.416

TABLE I: Upper and middle parts show the on-site Coulomb interaction U dependences of Fe_B-Fe_B bond lengths (in Å) in the corner sharing tetrahedra. The lower part shows valence charges q_d (in e) of Fe_B sites in $P2$ Fe_3O_4. In the middle table, B(3)-B(4) and B(4)-B(3) indicate *long* and *short* bond sides, respectively.

tion can only be determined up to an integer multiple of the polarization quantum [23]. In ferroelectric $P2$ Fe_3O_4 structure, the polarization quantum $e\boldsymbol{R}/\Omega$ is 16.12 $\mu C/cm^2$ along b direction, where e is the electron charge and $\boldsymbol{R}$ is the lattice vector along b.

Figure 6 shows polarizations along b obtained by point charge model and by the Berry phase method. In the later approach, the internal atomic positions of ferroelectric $P2$ and antiferroelectric $P2/c$ Fe_3O_4 are optimized in the conditions of U=4.5, 6.0, and 8.0 eV, and then the same U values as for the crystal optimizations are consistently used for polarization calculations. At U=4.5 eV, the polarization calculated by the Berry phase method is much larger than that of the point charge model. This large difference is due to strong enhancement of dipole moments by the Wannier centers displaced from atomic centers. Such enhancement of polarization is of course not taken into consideration in the point charge model. Additionally, calculated polarizations decrease when increasing the U value. The obtained results are consistent with the Fe_B^{2+}/Fe_B^{3+} bond dimerizations discussed in Sec.IV A. As increasing U, the Fe_B^{2+}/Fe_B^{3+} dimerizations are suppressed, so it can be easily understood that if the bond dimerization between Fe_B^{2+} and Fe_B^{3+} sites disappears, polarization caused by the site/bond-centered charge ordering vanishes. Another important point here is the polarization with large U values. As shown in Fig.6, polarizations calculated by the point charge model and the Berry phase method for large U approach the same value. This can be understood as follows: upon increasing U, electrons are more localized on Fe ions. Therefore, since the Wannier centers get closer to Fe_B sites and there is no enhancement of dipole moments by the displacements of the Wannier centers, the point charge model and the Berry phase method have similar values for large U.

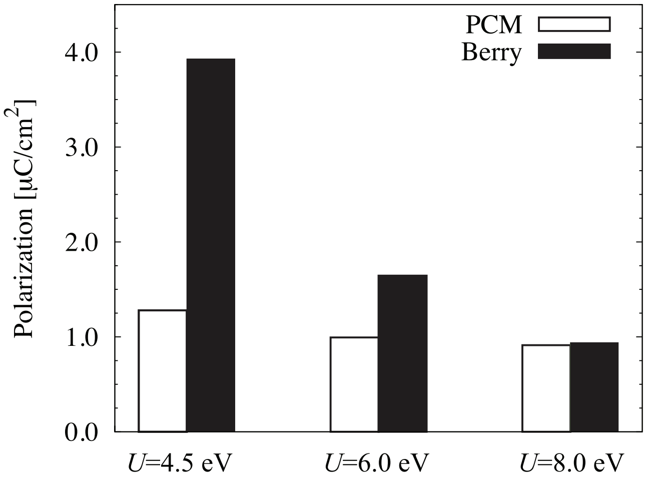

FIG. 6: Dependence of electric polarization P^b in ferroelectric $P2$ Fe_3O_4 on the on-site Coulomb interaction. Considered U values are 4.5, 6.0, and 8.0 eV. The exchange parameter J is fixed to 0.89 eV. Polarizations calculated by point charge model and by the Berry phase method are shown.

We now comment on the difference between our present results and our previous calculations. [11] We showed that Fe_3O_4 has Cc symmetry in the ground state and polarization direction is not along b but in the monoclinic ac mirror plane, P_{Berry}=(-4.41, 0, 4.12) in $\mu C/cm^2$ (for U=4.5 eV and J=0.89 eV). The difference between our present results and previous calculations originates from the microscopic mechanism of ferroelectricity: in Fe_3O_4 with Cc symmetry, the polarization is not driven by the site/bond-centered charge ordering but by "charge shift" at selected Fe_B sites. The bond dimerization on Fe_B^{2+} and Fe_B^{3+} sites along b in Cc Fe_3O_4 does indeed exist; however, dipole moments caused by the site/bond-centered charge ordering are cancelled between upper half and lower half of the unit cell, due to the Cc symmetry. Therefore, the site/bond-centered charge ordering is not appropriate as a mechanism of ferroelectricity in Cc magnetite.

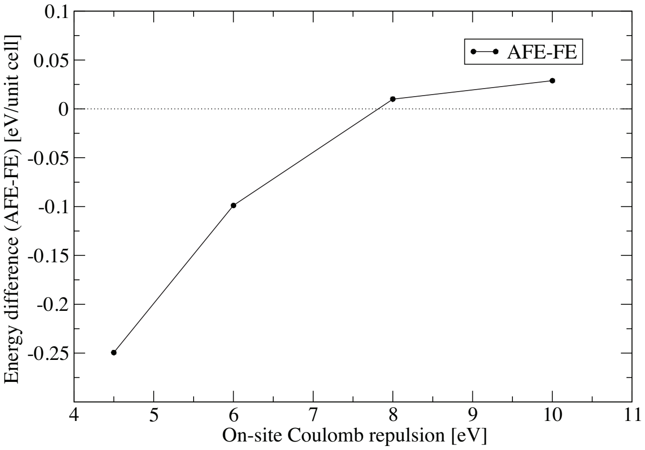

FIG. 7: On-site Coulomb interaction dependence of total energy difference per unit cell between antiferroelectric $P2/c$ (AFE) and ferroelectric $P2$ (FE) Fe_3O_4.

C. Stability of antiferroelectric $P2/c$ and ferroelectric $P2$ Fe_3O_4

Finally, we briefly discuss the stability of antiferroelectric $P2/c$ and ferroelectric $P2$ Fe_3O_4. Figure 7 shows the total energy differences per unit cell of antiferroelectric and ferroelectric Fe_3O_4 (after structural optimizations) as a function of on-site Coulomb interaction U. The structural optimizations are performed separately for ferroelectric and antiferroelectric Fe_3O_4 for U=4.5, 6.0. 8.0, and 10.0 eV. Incidentally, we note here that at U=4.5 eV, Fe_3O_4 with Cc symmetry is the ground state [11]. When the on-site Coulomb interaction is set to $U = 4.5$ eV, the ferroelectric state is less stable than antiferroelectric state as shown in Fig.7. However, the situation is changed for large U values. The energy difference between antiferroelectric $P2/c$ and ferroelectric $P2$ Fe_3O_4 decreases with increasing U value; when U reaches ~8.0 eV the ferroelectric state becomes even more stable than the antiferroelectric state, paving the way to $P2$ magnetite as a possible multiferroic.

V. SUMMARY

Microscopic mechanisms leading to Fe^{2+}_B/Fe^{3+}_B dimerization and ferroelectricity in Fe_3O_4 have been investigated by *ab initio* density functional theory with Hubbard U (GGA+U) method. From the on-site Coulomb interaction U dependence of Fe_B-Fe_B bond lengths in corner sharing tetrahedra, we show that the "asymmetric hybridization" between Fe^{2+}_B sites plays an important role in Fe^{2+}_B/Fe^{3+}_B bond dimerization, in addition to the simple inter-site Coulomb interaction. Additionally, based on the results of the U dependence of polarizations and Fe_B-Fe_B bond lengths, we show that the noncentrosymmetric Fe_3O_4 with $P2$ symmetry can become ferroelectric by means of the intermediate site/bond centered charge ordering proposed by Khomskii, where the Fe^{2+}_B/Fe^{3+}_B site charge order and Fe^{2+}_B/Fe^{3+}_B bond dimerization along the monoclinic b direction simultaneously occurs. $P2$ Fe_3O_4 can therefore be well considered as an *improper* multiferroic material with charge–order–induced ferroelectricity.

VI. ACKNOWLEDGMENTS

The research leading to these results has received funding from the European Research Council under the European Community's 7th Framework Programme (FP7/2007-2013) / ERC grant agreement n. 203523. We thank Prof. Daniel Khomskii for useful discussions. The crystal structures and the charge states are plotted by using the software VESTA [24].

---

[1] For comprehensive reviews, see S.W.Cheong and M.Mostovoy, Nature Mater.**6**, 13 (2007); R. Ramesh and N.A.Spaldin, Nature Mater. **6**, 21 (2007) and references therein.

[2] S. Picozzi and C. Ederer, J. Phys.: Condens Matter **21**, 303201 (2009).

[3] E. J. W. Verwey Nature (London) **144**, 327 (1939).

[4] E. J. W. Verwey and P. W. Haayman, Physica (Amsterdam) **9**, 979 (1941).

[5] P. W. Anderson, Phys. Rev. **102**, 1008 (1956).

[6] J. Garcia and G. Subias, J. Phys. Condens. Matter **16**, R145 (2004).

[7] J. P. Wright *et. al*, Phys. Rev. Lett. **87**, 266401 (2001).

[8] C. Medrano, M. Schlenker, J. Baruchel, J. Espreso, and Y. Miyammoto, Phys. Rev. B **59**, 1185 (1999).

[9] M. Alexe, M. Ziese, D. Hesse, P. Esquinazi, K. Yamauchi, T. Fukushima, S. Picozzi, and U. Gosele, Adv. Mater. **21**, 4452 (2009).

[10] D. Khomskii, Bull. Am. Phys. Soc. A13.00006 (2007); J. van den Brink and D. I. Khomskii, J. Phys.: Condens. Matter **20**, 434217 (2008).

[11] K. Yamauchi, T. Fukushima, and S. Picozzi, Phys. Rev. B **79**, 212404 (2009).

[12] J. P. Wright *et. al*, Phys. Rev. B **66**, 214422 (2002).

[13] G. Giovannetti and J. van den Brink, Phys. Rev. Lett. **100**, 227603 (2008).

[14] G. Kresse and J. Furthmuller, Phys. Rev. B **54**, 11169 (1996).

[15] J. P. Perdew *et. al*, Phys. Rev. Lett. **77**, 3865 (1996).

[16] S. L. Dudarev *et al.,* Phys. Rev. B **57**, 1505 (1998).

[17] H.-T. Jeng *et. al*, Phys. Rev. B **74**, 195115 (2006).

[18] Zuo *et. al*, Phys. Rev. B **42**, 8541 (1990).

[19] R. D. King-Smith and D. Vanderbilt, Phys. Rev. B **47**, 1651 (1993).

[20] R. Resta, Rev. Mod. Phys. **66**, 899 (1994).
[21] H.-T. Jeng *et. al*, Phys. Rev. Lett. **93**, 156403 (2004).
[22] I. Leonov, A. N. Yaresko, V. N. Antonov, M. A. Korot in, and V. I. Anisimov, Phys. Rev. Lett. **93**, 164404 (2004).
[23] J. B. Neaton *et. al*, Phys. Rev. B **71**, 014113 (2005).
[24] K. Momma and F. Izumi, J. Appl. Crystallogr. **41**, 653 (2008).